J Appl Electrochem (2011) 41:1087–1097
DOI 10.1007/s10800-011-0274-3

ORIGINAL PAPER

Electrochemical treatment of water containing chlorides under non-ideal flow conditions with BDD anodes

A. Vacca · M. Mascia · S. Palmas · A. Da Pozzo

Received: 3 December 2010 / Accepted: 23 February 2011 / Published online: 15 March 2011

Abstract In this work a undivided parallel plate cell equipped with boron doped diamond (BDD) anode was tested as electrochemical reactor for disinfection of water. Two configurations were adopted: a single pass configuration (SPC) and a recirculated configuration (RC) in which also a reservoir was inserted in the hydraulic circuit. In both the experimental configurations the system worked in continuous mode with a flow rate ranging from 0.05 to 0.42 $dm^3\ min^{-1}$; in the RC the recirculating flow rate ranged from 0.45 to 6 $dm^3\ min^{-1}$. Thermostated (25 °C) galvanostatic electrolyses were carried out with aqueous solutions containing 100 mg dm^{-3} of chloride ions: values of current density from 2.5 to 5.0 mA cm^{-2} were used. Steady state data revealed that active chlorine and chlorate ions were the main oxidation products. Particular attention was paid to the hydrodynamics both for SPC and RC: pulse-response curves were experimentally obtained with an inert tracer, and the behaviour of the system was interpreted by models based on a combination of ideal flow reactors, bypass flow elements, and dead zones. The hydrodynamic models were utilized to predict the outlet concentration of the electrolysis products. A good agreement between model predicted and experimental data was obtained for a wide range of experimental conditions. Preliminary disinfection tests were then performed using *Escherichia coli* as model microorganism. Results were discussed in terms of both disinfection efficiency and by-products formation.

A. Vacca (✉) · M. Mascia · S. Palmas · A. Da Pozzo
Dipartimento di Ingegneria Chimica e Materiali, Piazza d'Armi, Cagliari, Italy
e-mail: vacca@dicm.unica.it

Keywords Electrochemical treatment · Modelling · Hydrodynamics · Chlorates · Active chlorine

List of symbols

a	Specific electrode area [$a = \frac{A}{V}$ (m^{-1})]
A	Electrodic area (m^2)
C	Concentration (mol m^{-3})
D	Diffusivity coefficient ($m^2\ s^{-1}$)
d	Inter-electrode gap (m)
E(t)	Exit age distribution (s^{-1})
F	Faraday number (C mol^{-1})
H	Cell width (m)
h	Hydraulic diameter [$h = 4\frac{H\,d}{2\,(H+d)}$ (m)]
I	Current intensity (A)
i	Current density [$i = \frac{I}{A}$ (A m^{-2})]
k_d	Oxidants decay kinetic constant (s^{-1})
k_m	Mass transfer coefficient (m s^{-1})
N	Number of in-series tanks
p	Parameter in Eq. 2
q	Parameter in Eq. 2
Q	Electrolyte flow rate ($m^3\ s^{-1}$)
Q_R	Recirculating flow rate ($m^3\ s^{-1}$)
t_m	Mean residence time (s)
V	Electrolyte volume (m^3)
V_d	Dead zone volume (m^3)
V_R	Reservoir volume (m^3)
v	Linear velocity in the empty cell (m s^{-1})
z	Number of electrons
Re	Reynolds number ($Re = \frac{v\,h\,\rho}{\mu}$)
Sh	Sherwood number ($Sh = \frac{k_m\,h}{D}$)
Sc	Schmidt number ($Sc = \frac{\mu}{\rho\,D}$)
Pe	Peclet number ($Pe = \frac{v\,h}{D}$)
δ	Fraction of active volume

ε Faradic yield
Φ Overall fractional yield
μ Viscosity of electrolyte (kg m^{-1} s^{-1})
ρ Density of electrolyte (kg m^3)
σ^2 Variance of the peak
τ Hydraulic residence time (s)

Superscripts
a Anode
c Cathode

1 Introduction

Water disinfection is essential to prevent the spread of diseases caused by pathogens, thus the production of drinking water, restoration of groundwater, water treatment of swimming pool are just some examples of application areas for the processes of disinfection [1]. There are also emerging application fields as the protection of marine biodiversity through the disinfection of ballast waters [2]. Moreover, there is an increasing request for *easy to use* and mobile equipments to treat the waters in particular situations such as water supply for insulated or small communities and disinfection of water in emergency situations [3, 4].

Traditionally, chlorination is the most common method of disinfection thanks to the low cost, but its main drawback is the possible formation of trihalomethanes [5]. Other methods based on ozone and chlorine dioxide, which are in general more effective than chlorination, may lead to the formation of undesired disinfection by-products or may produce a poor persistent effect [6, 7]. Another important problem that affects the chemical disinfection is the hazard connected to producing, transporting and handling large amounts of such substances as chlorine and ozone [8].

Electrochemical processes are often involved in disinfection, because most of the disinfectant compounds are produced electrochemically. So, the direct application of the electrochemical disinfection can represent an intensification of the process [9]. Moreover, the electrochemical treatment presents other attractive peculiarity such as the versatility of the process and the simplicity of the reactors in terms of construction and management, which makes it particularly suitable for automation.

As reported by several authors, during the disinfection of water by direct electrolysis several products and by-products may be formed with different disinfecting ability [10, 11]: the so-called mixed oxidant shows a disinfecting ability higher than the addition of a single chemical, also thanks to the possible presence of short-life radical species [12].

The high bactericidal effect of the electrochemical treatment was also attributed to the combined effect of mixed oxidants, electric field and pH gradients in the reactor [13–16].

Similarly to other treatments, also the electrochemical disinfection may lead to the formation of different by-products (DPBs) [17–20]. Among them, chlorates are of great concern because the effect of these compounds on the human health is still under study: they are suspected to have health risks so that the WHO recommends very low concentrations of ClO_3^- and ClO_4^- in drinking water [21].

A correct choice of anode material and operative conditions are key parameters to obtain a powerful mixture of disinfectant limiting the production of DPBs. Boron doped diamond (BDD) anodes could be an excellent candidate due to its capability to form very powerful disinfecting agents [22, 23]; moreover BDD presents other interesting properties such as chemical inertness and stability [24].

The composition of the water to be treated is a crucial point, with particular regard to the presence of chlorides. These species show a contrasting effect during electrolysis: Cl^- can be oxidised to active chlorine species (dissolved chlorine, hypochlorous acid and hypochlorite ions) with beneficial disinfecting effects; on the other hand different undesired DPBs as chlorite, chlorate and perchlorate ions may be formed. Recently, Bergmann and coworkers [10, 25] highlighted the risk of formation of chlorate and perchlorate ions during electrolysis by using BDD anodes.

In this context, an experimental work started in our laboratory on electrochemical treatment of natural and wastewater and the related products obtained during the process [20]: the presence of chlorite, chlorate and perchlorate ions was found during electrolyses of solution containing chloride at BDD anode, together with a mixture of oxidising species mainly constituted by active chlorine. Attention was paid on the study of the oxidation mechanism of chloride ion at BDD anodes, in order to handle main effects of the involved reactions from an engineering viewpoint, and the simplified model in Fig. 1 was proposed.

Following the proposed mechanism, oxidation of chloride occurs at the anode surface to give chlorine, with a faradic yield ε_1, as well as the first step of water oxidation to form OH radicals [26]. The dissolved chlorine, electrochemically formed, reacts with water to hypochlorous acid and hypochlorite. The distribution between the three main active chlorine components is strongly dependent on pH. A fraction $\alpha\varepsilon_2 i$ of the OH radicals can be involved in a series of reactions to give oxygen and reactive oxygen species as ozone and hydrogen peroxide [27]. Chlorine can react with a fraction $\beta\varepsilon_2 i$ of OH radicals to give chlorine dioxide and more oxidised chlorine species as chlorates. When the chemistry near the electrode is dominated by radical mechanisms characterized by rate constants in the range of 10^5–10^{10} $mole^{-1}$ m^3 s^{-1}, those mechanisms would replace

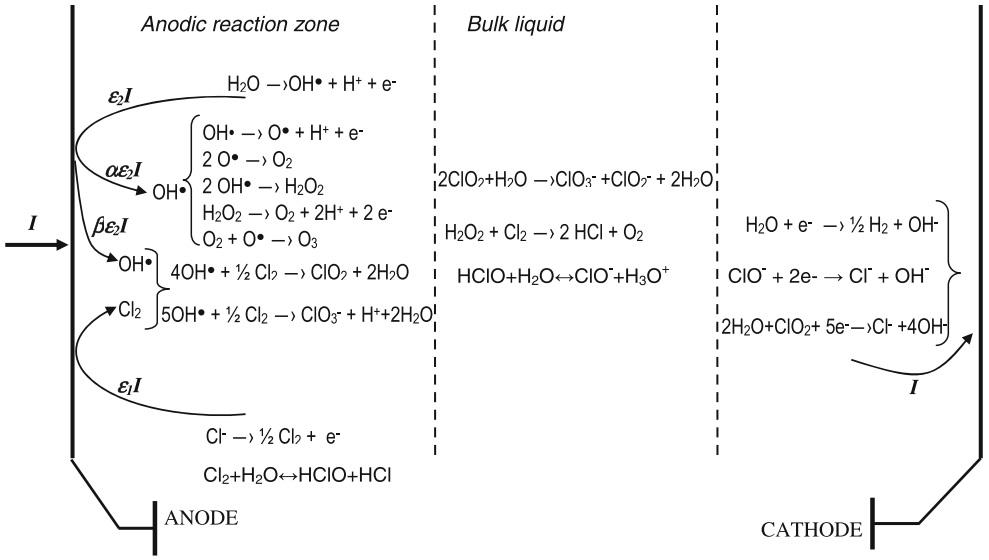

Fig. 1 Scheme of the chemical and electrochemical reactions

the known reaction paths, based on the electrochemical oxidation of hypochlorite or chloride to chlorate [28, 29]. As it was suggested by Ibl and Landolt [28] at the lower pH near to the anode, the chlorine hydrolysis moves progressively into the bulk solution where the pH is higher, so that the hypochlorite concentration increases in the bulk solution, and back diffusion towards the anode is produced. Hypochlorite ions act as proton acceptors in the acidic diffusion layer, increasing the pH and promote chlorine hydrolysis. Under these conditions, only part of the hypochlorite ions diffusing towards the anode are oxidized electrochemically. Czarnetzki and Janssen [29] proposed the direct electrochemical oxidation of chloride to chlorate without a dissolved hypochlorite species as intermediate at RuO_2/TiO_2 anodes. Also possible reactions between the electrochemically produced oxidants were considered to take account for a decrease in the amount of active chlorine formed. Chlorate and chlorite ions can be formed also from the disproportionation of chlorine dioxide. The chlorite ions can rapidly react to give chlorates so that, as it was suggested from the literature [25], only traces of these species are formed.

At the cathode the reduction of the oxidants often occurs under mass transfer control along with the hydrogen evolution. The distribution of the oxidation by-products depends on mass transfer, current density and chloride concentration [20].

As the disinfection is concerned, the concentration of oxidants is not the only relevant parameter for the efficiency of the process, which also depends on the contact time of the bacteria with the specific disinfectant agent [30].

In a continuous system under non ideal flow conditions, distribution of residence times and oxidant concentrations and, in turn, the hydrodynamics of the system must be considered. This is of particular concern in an electrochemical reactor where the oxidants are produced along the cell and react both at surface and in the bulk of the solution.

Reactors are often designed under the hypothesis of ideal flow conditions, such as completely stirred reactor (CSTR) and perfect plug flow reactor (PFR). However, the real flow pattern inside the treatment unit normally presents dispersion phenomena, dead or stagnant zones, bypass flows, exchanges between them and recirculation zones that can affect the efficiency of the process [31].

In the electrochemical disinfection process dead zones may result in long reaction time, favouring the bulk reactions to form chlorates, whereas by-pass may cause contact times lower than the hydraulic residence time, leading to overestimate the disinfection efficiency. The hydrodynamic behaviour of non ideal reactors can be interpreted using models consisting in a combination of plug-flow zones, ideally mixed zones, by-pass flow elements, and dead zones; the parameters of these combined models can be obtained by the residence time distribution (RTD) curves [32].

In this context, the aim of this work was to investigate the performances of a parallel plate reactor as electrochemical cell for water disinfection processes. The mass transfer within the cell was characterised by the limiting current density technique, whereas the hydrodynamics was studied by pulse response experiments. The effects of the operative conditions and the hydrodynamic behaviour of

the system on the composition of the outlet stream were numerically simulated by a model. The model predictions were compared with the experimental results.

2 Materials and methods

2.1 Experimental apparatus and procedures

Electrolyses were performed in a single compartment cell (EC Electro MP-Cell) with two parallel plate electrodes. The main cell dimensions were 12 cm × 18 cm with an interelectrode gap of 0.5 cm. The gap was filled with a polyethylene grid as turbulence promoter: details of the anode side with the turbulence promoter are shown in Fig. 2. p-type semiconducting boron- doped diamond (boron concentration in the range 3,500–5,000 ppm), supplied by ADAMANT, was used as anode (diameter 10 cm; thickness 0.5 cm). It was prepared by hot filament chemical vapour deposition (HFCVD) on a low resistivity silicon wafer. Stainless steel (AISI 304) was used as cathode. The anodic and cathodic areas were 80 cm^2. The cell was used in two configurations (Fig. 2): single pass (SPC) and recirculated system (RC). In SPC the cell (Fig. 2a), operating in continuous mode, was fed by a peristaltic pump: the electrolyte flowed throughout the cell in a single pass mode with flow rates (Q) ranging from 0.05 to 0.42 dm^3 min^{-1} which corresponded to Reynolds numbers equal to 15 and 105, respectively. The volume of the system was 40 cm^3 and the hydraulic residence time ($\tau = V/Q$) in the electrochemical system ranged from 0.12 to 1.0 min.

In the RC configuration the cell was inserted in a hydraulic circuit (Fig. 2b) in which the electrolyte was pumped by a centrifugal pump from the reservoir to the cell and back with recirculating flow rates (Q_R) ranging from 0.45 to 6 dm^3 min^{-1}. Also in this case the whole system (cell and reservoir) operated in continuous mode: a peristaltic pump was used to independently feed the reservoir with the same flow rates (Q) used for SPC. In this case the Reynolds number of the cell ranged from 120 to 1,550. The total volume of the system was 850 cm^3 and the hydraulic residence time in the electrochemical system ranged from 1.1 to 16 min.

The cell temperature was controlled by a thermostatic bath at 25 ± 2 °C.

The electrolyses were performed by imposing current density values ranging from 2.5 to 5.0 mA cm^{-2} by means of a galvanostat (AMEL-2049). All the experiments were carried out with solutions containing 200 mg dm^{-3} of SO_4^{2-} as supporting electrolyte and 100 mg dm^{-3} of Cl^-, both as sodium salts.

The outlet stream of the system was analysed for the concentration of reactant and products during the experiments: only steady state data were considered for the discussion.

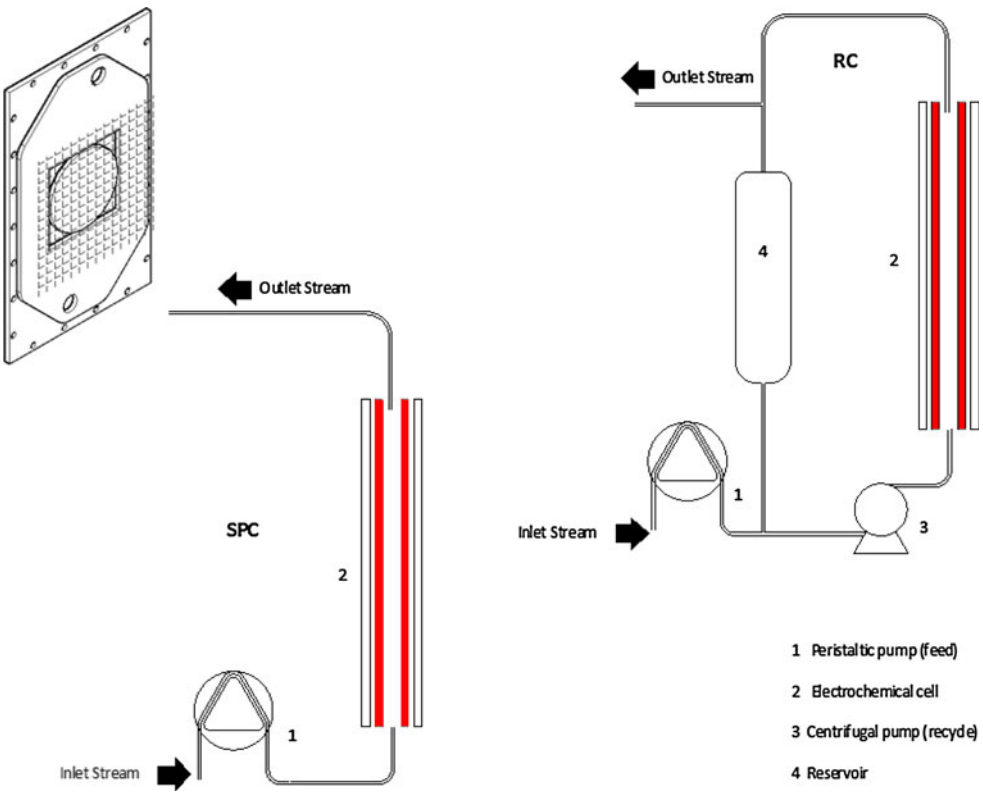

Fig. 2 Schematic view of the two experimental configurations with a detail of the cell

In the disinfection experiments the inlet stream contained suitable amounts of *Escherichia coli* ATCC 25922. The bacterial strains were grown in BHI broth (Difco Laboratories, Detroit, MI) for 24 h at 37 °C. Inlet concentration of *E. coli* was about 1×10^4 CFU/mL (Colony Forming Unit/mL).

2.2 Analyses

During the runs samples were withdrawn and analysed for the concentration of reactant and products: since some components may have very short live times, the analysis were done immediately after sampling.

The oxidant concentrations expressed as mg dm^{-3} of active chlorine were measured by *N*,*N*-diethyl-*p*-phenylenediamine (DPD) colorimetric method: DPD is oxidized to form a red-violet product, the concentration of which is determined reflectometrically (ASTM 4500 G). Hypochlorite concentration was determined by spectrophotometric analysis in the UV region at 292 nm [33]. The molar absorptivity at 292 nm is 362 ± 5 dm^3 mol^{-1} cm^{-1} at pH = 10. Chlorine dioxide was measured spectrophotometrically by red chlorophenol method: with this method the literature reports no interferences in the determination of chlorine dioxide down to 0.5 mg dm^{-3} in the presence of chlorite, hypochlorite and chlorate [34]. The spectrofotometric determinations were done with Spectrophotometer VARIAN—Cary 50. Ion concentrations were measured by a Metrohm compact ion chromatograph 761 equipped with conductivity detector and 6.1006.430 Metrosep Anion supp. 4 column, (mobile phase 2 mM $NaHCO_3$/1.3 mM Na_2CO_3, flow rate 1.5 cm^3 min^{-1}). In particular, ion chromatography was effectively used to measure the concentration of Cl^-, ClO_3^- and ClO_4^-, as well as possible variations in the SO_4^- concentration. Analyte identification was accomplished on the basis of the retention times of the analytes and the quantification was performed by external calibration. As far as the concentration of hypochlorite was concerned, some problems arose since chloride and hypochlorite have overlapping peaks. As suggested by Bergmann [25], the analysis was carried out twice with and without hypochlorite elimination and the corresponding concentration values calculated by solving a mathematical system of equations. Indication on the actual concentration of hypochlorite was also derived from the UV spectrum measurements.

N,*N*-diethyl-*p*-phenylenediamine method gave a measure of the active chlorine, as global concentration of oxidising species contained in the sample: ClO^-/HClO, ClO_2, but also H_2O_2, O_3 and persulphate can be evaluated with this measure. In our case, most of the oxidant is constituted by ClO^-/HClO as demonstrated by the analysis of analogous samples performed with DPD method and UV spectrum.

In order to determine the concentration of microorganisms in the inlet and outlet streams, the microbial suspensions were inseminated in Cled agar and incubated at 37 °C. After 48 h the microbial colonies were counted. Each sample was cultured in triplicate.

2.3 Hydrodynamic and mass transfer characterization

To characterize the mass transfer behaviour of the cell, the well established limiting-current technique was adopted [35], so that the value of mass transfer coefficient (k_m) was derived (Eq. 1) from the limiting current density i_L, measured at the working electrode when the mass transfer conditions where achieved:

$$k_m = \frac{i_L}{zFC} \tag{1}$$

In the specific case mass transfer coefficients were determined by evaluating the related limiting current densities for the ferro/ferricyanide redox couple (supporting electrolyte 0.5 M Na_2CO_3). In particular, the determination of the anodic mass transfer coefficient (k_m^a) was made by measuring the limiting current densities for $K_4Fe(CN)_6$ 1 mM oxidation in the presence of an excess of $K_3Fe(CN)_6$ (0.1 M) in order to ensure that the cathodic reaction never became the limiting process.

The values of mass-transfer coefficients were used to obtain mass-transfer correlations in the form

$$\mathrm{Sh} = \mathrm{p}\ \mathrm{Re}^{\mathrm{q}}\mathrm{Sc}^{0.33} \tag{2}$$

where p and q are fitting parameters, and the 0.33 power of the Schmidt number was assumed a priori. To evaluate the dimensionless numbers, the physical properties of ferrocyanide solutions (kinematic viscosity $v = 0.952 \times 10^{-6}$ m^2 s^{-1} and diffusion coefficient $D = 6.41 \times 10^{-10}$ m^2 s^{-1}) were used. The values of p and q obtained are 0.49 and 0.51 respectively: the value of q is quite similar to the values reported for the turbulent flow in parallel plate systems, even if the Reynolds numbers are very low [36]. Similar results are reported in the literature for several parallel plate reactors, and were attributed to the entrance effects and to the presence of turbulence promoters [37, 38].

The hydrodynamic characterization was performed by pulse-response tests, which involves the injection of a tracer at the inlet of the system and the recording of the concentration–time curve C(t) at the outlet. To this aim a sharp pulse of tracer (KCl 3 M) was injected upstream of the system while a conductivity detector, located at the outlet, allowed to record the passage of the tracer, and in turn to evaluate the RTD. The analysis of the experimental RTD has been done calculating the following parameters:

(1) Exit age distribution E(t)

$$E(t) = \frac{c(t)}{\int_0^\infty c(t)dt} \tag{3}$$

(2) Mean residence time

$$t_m = \frac{\int_0^\infty t\, c(t)dt}{\int_0^\infty c(t)dt} \tag{4}$$

(3) Variance

$$\sigma^2 = \frac{\int_0^\infty (t-\tau)^2\, c(t)dt}{\int_0^\infty c(t)dt} \tag{5}$$

3 Results and discussion

Figure 3 shows the concentrations of oxidants and chlorates in the outlet stream at the steady state. The concentrations of oxidants are reported as mM of active chlorine as obtained by the DPD method: as already reported in the experimental section, the main oxidising agent was hypochlorite. The experiments were performed under different operative conditions and with different reactor configurations at a fixed concentration of chloride of 100 mg dm^{-3}, that is typical of a natural water. However, since the values of the specific area *a* involved in the two systems are different in the two configurations (a = 200 m^{-1} for SPC; a = 9.5 m^{-1} for RC), data in Fig. 2 are reported as a function of the parameter aτ. It is worth to highlight that, in this way, the lowest aτ correspond to SPC. As can be seen in the figure, low concentrations of chloride oxidation products correspond to low values of aτ, i.e. to SPC.

The distribution of these products was strongly dependent on Re number and current density.

Oxidants and chlorates were the only species detected in the outlet stream under all the experimental conditions investigated. During electrolyses with BDD anodes the possible formation of chlorite and perchlorate ions is discussed in the literature: chlorite ions are intermediates of chlorate formation [29, 39] but they are short-lived compounds, while the formation of perchlorate by the further oxidation of chlorate only occurs at high values of current density [20].

As the overall fractional yield (Φ) of the oxidants is concerned, Fig. 4 shows the results obtained during electrolyses in the recirculated system under different operative conditions. The overall fractional yield was defined as:

$$\Phi = \frac{C_{out}^{ox}}{C_{in}^{Cl^-} - C_{out}^{Cl^-}} \tag{6}$$

As can be seen, Φ increased with Re, but the effect was less relevant at high Re numbers. At the anode an increase in the mass transfer rate allows a fast transport of electrogenerated oxidants to the bulk, so limiting the further oxidation to chlorate by OH radicals in the anodic zone. On the other hand, at the cathode, an increase in the Re number increases the mass transfer rate of oxidants toward the cathode, which is the controlling step of the reduction rate. Due to the geometry of the cell the two transfer rates depend in the same way on Re, so that the resulting concentration of oxidants is scarcely influenced

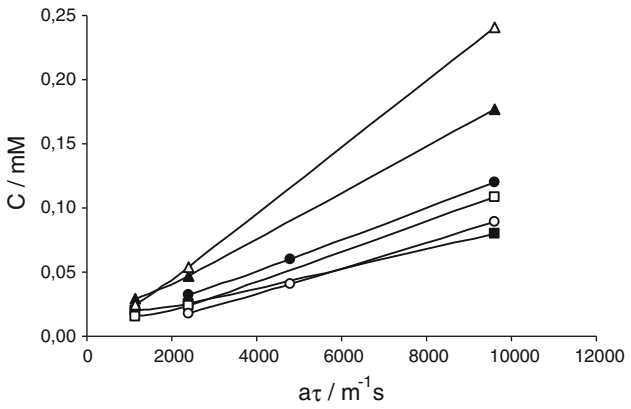

Fig. 3 Trend with aτ of oxidising species (*filled symbols*) and chlorate (*open symbols*) concentrations, during electrolysis under different experimental conditions: (*filled square*, *open square*) Re = 120, i = 2.5 mA cm^{-2}; (*filled triangle*, *open triangle*) Re = 120, i = 5.0 mA cm^{-2}; (*filled circle*, *open circle*) Re = 360, i = 2.5 mA cm^{-2}

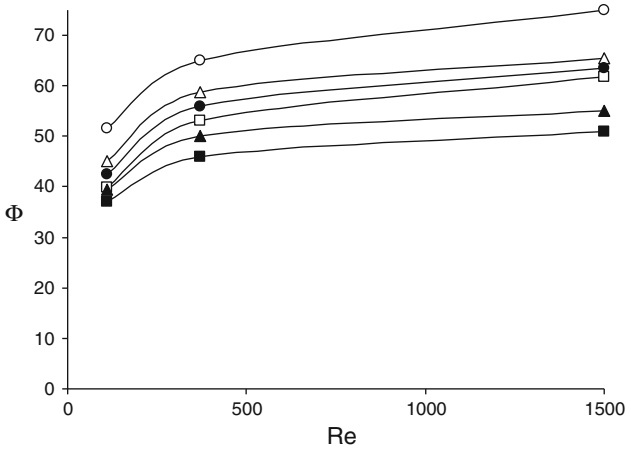

Fig. 4 Overall fractional yield of the process as a function of Re number obtained during electrolysis in the RC for t = 4 min (*open symbols*) and t = 16 min (*filled symbols*): (*filled circle*, *open circle*) i = 2.5 mA cm^{-2}; (*filled triangle*, *open triangle*) i = 3.7 mA cm^{-2}; (*filled square*, *open square*) i = 5.0 mA cm^{-2}

at high Re number when the transport phenomena are predominant.

Moreover, an increase in the current density leads to higher current of OH radical formation in the reaction zone, since the current for oxidation of chloride is scarcely affected by current density. This in turn increases the OH radicals available to react with chlorine to form chlorates, decreasing Φ.

Similar results were obtained with the SPC, as it can be observed in Fig. 5.

As in the case of RC, the increase in current density led to a decrease in the overall fractional yield. Although the concentrations of oxidants and chlorate increased with the hydraulic residence time, the values of Φ were lower. This behaviour may be explained considering that high Φ values can be obtained at high values of Re, which correspond to low residence times. Comparing the overall fractional yield obtained in the different experimental configurations, SPC shows highest values of Φ, the current density being the same. This behaviour seems to be connected with the low residence time, which is achieved in the single pass cell, but also the different hydrodynamics of the systems have to be taken into account.

Figure 6 shows the RTD data experimentally obtained for different inlet flow rates in SPC; as can be seen a well shaped single peak was always obtained with moderate tailing. At the lower flow rates, the concentration peak was smaller and the curves wider, indicating higher mixing levels.

In order to numerically interpret the behaviour observed, two types of dispersed models can be used: the *axial dispersed plug flow* model and the *stirred tank-in-series* model [40]. Table 1 shows the results of the statistic moment analysis for each flow rate, along with the characteristic parameters of the hydrodynamic models calculated by the following equations [41]:

$$\frac{\sigma^2}{t_m^2} = \frac{2}{Pe} - \frac{2}{Pe^2}\left(1 - e^{-Pe}\right), \quad N = \frac{t_m^2}{\sigma^2} \tag{7a, b}$$

As it would be expected, when the flow rate decreases the dispersion effects increase, as well as the number of CSTR needed.

It is well know that both models can be used to represent experimental curves with one peak and moderate tailing. Moreover, the two models are equivalent when N ≈ Pe/2 + 1, as it was in our case [40]. However, for reaction orders other than one and for multiple reactions, the *tanks-in-series* model is mathematically easier to use to obtain the effluent concentration and the conversion.

In Fig. 6 the RTD function E(t) calculated using N CSTR-*in-series* model is reported. The distribution function was calculated by:

$$E(t) = \frac{t^{N-1}}{(N-1)!\tau_i^N} e^{-t/\tau_i} \tag{8}$$

The curves fit well the E(t) data for all the flow rates examined, indicating that the N CSTR model is adequate to interpret the hydraulic behaviour of the system.

As RC was considered, the RTD curves showed a long tail, as expected for a recycle reactor, and for all the recirculating flow rates the obtained responses clearly indicated the existence of a dead zone. In order to interpret this behaviour a model was adopted in which the tanks in series representing the cell were combined with a reservoir modelled by a CSTR with dead zone (V_d). Figure 7 shows the sketch of the adopted model along with an example of RTD function E(t) obtained for RC. The E(t) function was numerically modeled by Matlab using Laplace transform technique. Values of dead volume fraction of 40 and 60% and exchange flow rates of 0.14 and 0.42 $dm^3\ s^{-1}$ were obtained by sensitivity

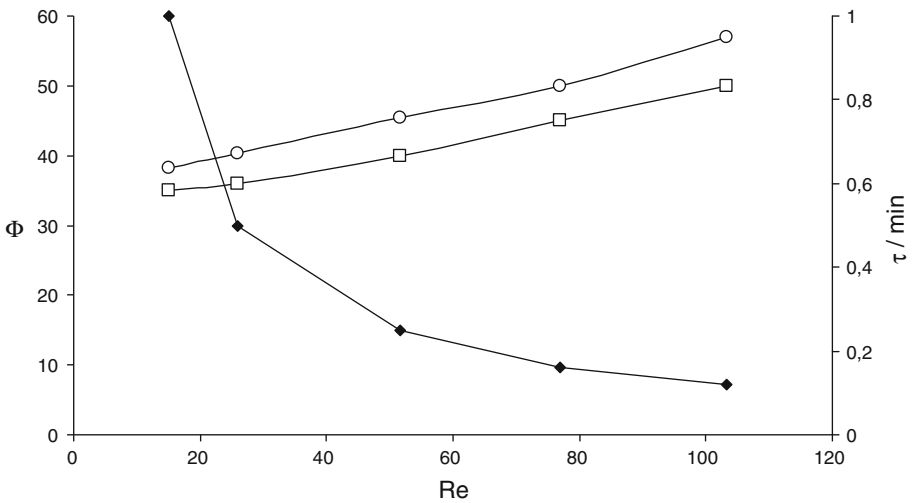

Fig. 5 Overall fractional yield of the process (*open symbols*) as a function of Re number obtained during electrolysis in the SPC: (*open circle*) i = 2.5 mA cm^{-2}; (*open square*) i = 5.0 mA cm^{-2}. *Filled symbols* represent the hydraulic residence time for each Re number

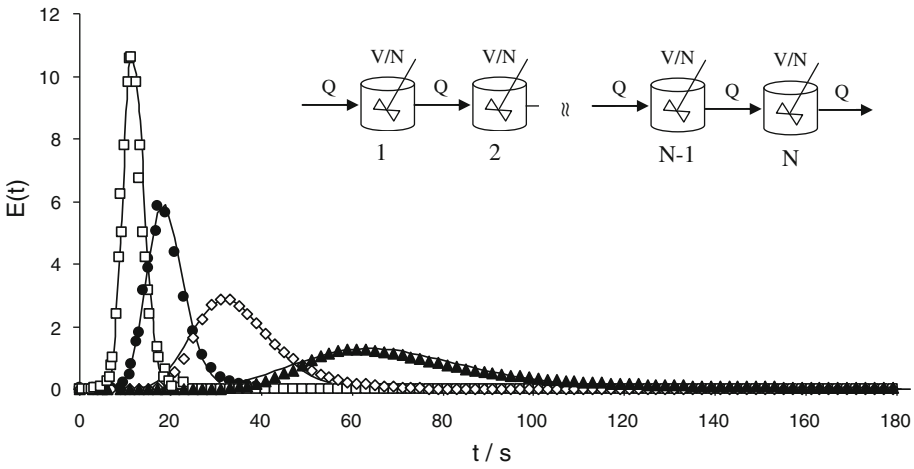

Fig. 6 Comparison of model simulation for N *tanks-in-series* model of E(t) distribution with experimental observations at SPC. *Open square* Re = 100; *filled circle* Re = 75; *open diamond* Re = 50; *filled triangle* Re = 15

Table 1 Parameters of the RTD curves of SPC

Q (dm^3 min^{-1})	Re	t_m (min)	σ^2 (min^2)	Pe	N
0.01	3	5.56	5.6633	9.2	5
0.02	6	2.52	0.9597	12.7	6
0.04	12	1.31	0.2531	14.1	7
0.08	24	0.61	0.0260	27.2	14
0.12	36	0.43	0.0120	30.0	16
0.20	60	0.27	0.0033	40.8	22
0.28	84	0.20	0.0014	54.1	28
0.36	102	0.18	0.0009	68.4	35

analysis, for recirculating flow rate of 0.4 and 1.4 dm^3 min^{-1}, respectively.

The hydrodynamic model of the system was then used to obtain a mathematical description of the process at the steady state. For SPC the mass balance for oxidants at the i-th reactor at the steady state can be written as follow:

$$Q\left(C_i^{ox} - C_{i-1}^{ox}\right) = \frac{iA_i^a}{zF}(\varepsilon_1 - \varepsilon_2) - A_i^c k_m^c C_i^{ox} - k_d C_i^{ox}\frac{V}{N} \quad (9)$$

The first term in the right side represents the net formation of oxidants at the anode surface, which accounts for the faradic yields of the oxidation of chloride (ε_1) and of the consumption of oxidants due to their further oxidation to form chlorate (ε_2). The second and the third terms represent the cathodic reduction of the oxidants, which was considered under mass transfer control, and the deactivation of active chlorine in the liquid phase, respectively.

The mass balance for the chlorate ions can be written as:

$$Q\left(C_i^{ClO_3^-} - C_{i-1}^{ClO_3^-}\right) = \frac{iA_i^a}{zF}\varepsilon_2 + k_d C_i^{ox}\frac{V}{N} \quad (10)$$

Equations 9 and 10 can be solved to calculate the concentration of each species in the outlet stream of the i-th reactor:

$$C_i^{ox} = \frac{C_{i-1}^{ox} + \frac{\tau}{N}\frac{ia^a}{zF}(\varepsilon_1 - \varepsilon_2)}{1 + \frac{\tau}{N}\left(a^c k_m^c + k_d\right)} \quad (11)$$

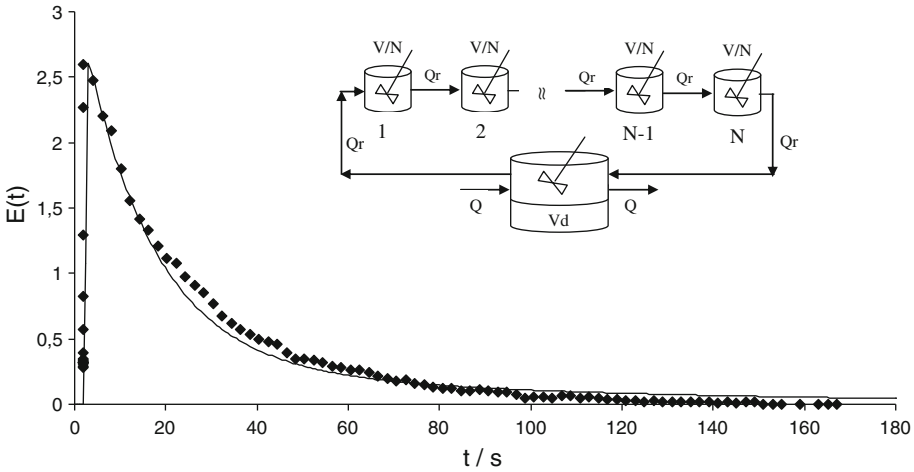

Fig. 7 Comparison of model simulation for N *tanks-in-series* model combined with CSTR with dead zone of E(t) distribution with experimental observations at RC. Re = 360

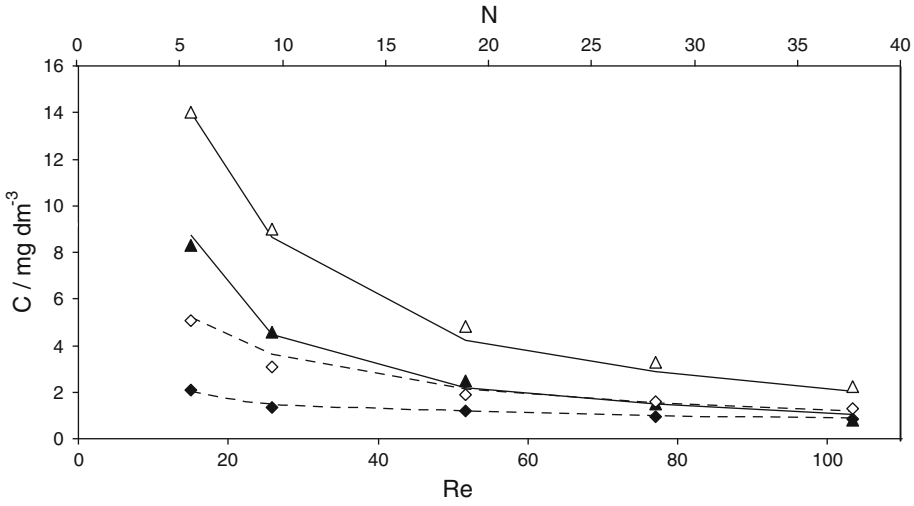

Fig. 8 Comparison between experimental (*symbols*) and model predicted data (*lines*) obtained at SPC for oxidants (*open diamond*, *filled diamond*) and chlorate (*filled triangle*, *open triangle*) concentrations as a function of Re. i = 2.5 mA cm^{-2} (*filled symbols*); i = 5.0 mA cm^{-2} (*open symbols*)

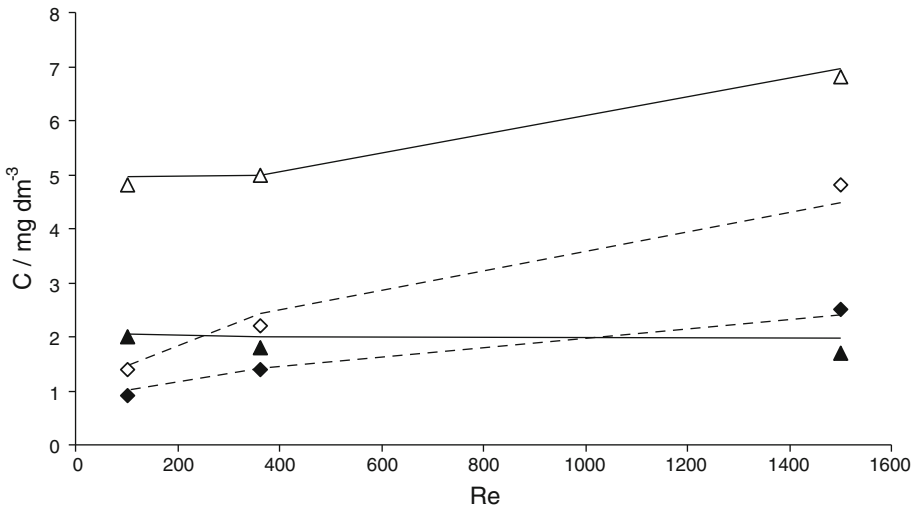

Fig. 9 Comparison between experimental (*symbols*) and model predicted data (*lines*) obtained at RC for oxidants (*open diamond*, *filled diamond*) and chlorate (*filled triangle*, *open triangle*) concentrations as a function of Re. i = 2.5 mA cm^{-2} (*filled symbols*); i = 5.0 mA cm^{-2} (*open symbols*)

Table 2 Inactivation of *E. coli* in 200 mg dm^{-3} SO_4^{2-} + 100 mg dm^{-3} of Cl^- under different experimental conditions

Configuration	Q (dm^3 min^{-1})	Re	N_{in}/N_{out}	C_{ox} (mg_{Cl_2} dm^{-3})	ClO_3^- (mg dm^{-3})
SPC	0.28	84	0.075	0.33	0.98
SPC	0.36	102	0.150	0.30	0.81
RC	0.10	360	N.D.	1.40	1.42
RC	0.40	360	N.D.	0.70	0.82

Initial *E. coli* concentration 1×10^4 CFU/mL

$$C_i^{ClO_3^-} = C_{i-1}^{ClO_3^-} + \frac{\tau}{N}\left(\frac{ia^a}{zF}\varepsilon_2 + k_d C_i^{ox}\right) \quad (12)$$

The specific reaction rate for the deactivation of the oxidants k_d was a fitting parameter: a good agreement with the experimental data was obtained with a value of 6×10^{-4} s^{-1}, which is similar to that experimentally evaluated in a previous work [20]. Values of ε_1 ranging from 0.047 to 0.09 and ε_2 (0.03) in Eqs. 11–12 were evaluated as described in a previous work [20]. The values of cathodic mass transfer coefficients were calculated by Eq. 2 at the relevant Re numbers ($\nu = 0.952 \times 10^{-6}$ m^2 s^{-1}; $D = 1.05 \times 10^{-9}$ m^2 s^{-1} [42]).

The comparison between experimental and model predicted data is showed in Fig. 8, where the concentrations of active chlorine species and chlorate ions are reported as a function of Re. As can be seen the model describes well the composition of the outlet stream under all the operative conditions investigated.

Considering RC, the mass balances at steady state for oxidants and chlorate can be written by combining equations 11 and 12 with the mass balance in the reservoir:

$$C_{out}^{ox} = \frac{C_N^{ox} Q_R}{Q + Q_R + \delta V_R k_d} \quad (13)$$

$$C_{out}^{ClO_3^-} = \frac{\delta V_R k_d C_{out}^{ox} + Q_R C_N^{ClO_3^-}}{Q + Q_R} \quad (14)$$

where C_N^i is the concentration of the species in the outlet of the N-th reactor and δ is the fraction of active volume.

Equations 11–14, were numerically solved to obtain the composition of the outlet stream at the steady state. Figure 9 shows the comparison between the relevant experimental and model predicted data; as can be seen, also in this case the model interprets well the concentration of oxidants and chlorates.

Preliminary disinfection tests were carried out by using *E. coli* as model microorganism: experiments were performed with an initial concentration of 10^4 CFU/mL of *E. coli*. The results are summarised in Table 2: a total removal of the bacteria was achieved under all the operative conditions with the RC. However, a concentration of chlorates of 2 mg dm^{-3} was obtained, which is higher than the recommended values of standard quality for water (0.8 mg dm^{-3}) [21]. This can be attributed to the high residence times, which lead to high removal of bacteria but allow high contact times for the oxidation of active chlorine species to chlorates.

With SPC the effectiveness of disinfection was still high, although the contact times are very low; this resulted in a concentration of chlorates below the recommended value [21]. The high effectiveness may be attributed to the synergetic effect of different mechanisms: in addition to the simple disinfection by active chlorine, the application of the electric field is harmful for the cell membrane; moreover, high local concentrations of reactive oxygenated species and transient of water can be achieved near the anode surface, favouring a fast killing of the microorganisms [20, 22].

4 Conclusions

The electrolysis of water containing chlorides under non ideal flow conditions with BDD anodes was investigated under steady state conditions. High production of oxidants was observed, while chlorates were found as main electrolysis by-products.

The hydrodynamics of the two configurations was characterised and modelled, and the hydrodynamic model was combined with the kinetics of the process to obtain a numerical representation of the system. The combined model effectively represents the behaviour of the process under all the experimental conditions considered, allowing to obtain information on several crucial issues:

- The concentrations of oxidants and by-products in the outlet stream can be easily predicted
- The distribution of contact times and oxidants concentration can be calculated, which is of particular concern in the disinfection processes
- The optimal operative conditions can be identified to maximise the generation of oxidants and limit the formation of chlorates.

The proposed electrochemical process can be very effective for disinfection of natural waters: preliminary disinfection tests showed good effectiveness in the inactivation of *E. coli*, exploiting the synergic effect of oxidants, chlorinated and oxygenated, and electric field.

Acknowledgments This research was supported by grants from the Italian Ministry of University and Scientific Research (PRIN 2008).

References

1. Chong MN, Jin B, Chow CWK, Saint C (2010) Water Res 44:2997
2. Kornmueller A (2007) Water Sci Technol 55(12):1
3. Hunter PR (2009) Environ Sci Technol 43:8991
4. Mazumdar N, Chikindas ML, Uhrich K (2010) J Appl Polym Sci 117:329
5. Mosteo R, Miguel N, Martin-Muniesa S, Ormad MP, Ovelleiro JP (2009) J Hazard Mater 172:661
6. Delaed TJ (2006) Microbiol Res 163:192
7. Singer PC (1994) J Environ Eng 120:727
8. Kraft A (2008) Platin Met Rev 52:177
9. Ghernaout D, Ghernaout B (2010) Dessaline Water Treat 16:156
10. Bergmann MEH (2009) Electrochim Acta 54:2102
11. Bergmann MEH, Koparal AS (2005) J Appl Electrochem 35:1321
12. Bergmann MEH, Koparal AT, Koparal AS, Ehrig F (2008) Microchem J 89:98
13. Pérez G, Gómez P, Ibañez R, Ortiz I, Urtiaga AM (2010) Water Sci Technol 62:892
14. Ghernaout D, Badis A, Kellil A, Ghernaout B (2008) Desalination 219:118
15. Gaskova D, Sigler K, Janderova B, Plasek J (1996) Bioelectrochem Bioenergy 39:195
16. Drees KP, Abbaszadegan M, Maier RM (2003) Water Res 37:2291
17. Gao Y (1997) WLB, Wasser Luft Boden 41:25
18. Hamm B (2002) Water Cond Purif 44:24
19. Son HJ, Cho M, Kim JE, Oh BT, Chung HM, Yoon JY (2005) Water Res 39:721
20. Polcaro AM, Vacca A, Mascia M, Palmas S, Rodriguez Ruiz J (2009) J Appl Electrochem 39:2083
21. World Health Organization (WHO) (2008) Guidelines for drinking water quality, 3rd edn. WHO Press, Geneva
22. Polcaro AM, Vacca A, Mascia M, Palmas S, Pompei R, Laconi S (2007) Electrochim Acta 52:2595
23. Jeong J, Kim JY, Yoon J (2006) Environ Sci Technol 40:6117

24. Panizza M, Michaud PA, Cerisola G, Comninellis C (2001) Electrochem Commun 3:336
25. Bergmann MEH, Rollin J (2007) Catal Today 124:198
26. Gandini D, Michaud PA, Duo I, Mahe E, Haenni W, Perret A, Comninellis C (1999) New Diam Front Carbon Technol 9:303
27. Marselli B, Garcia-Gomez J, Michaud PA, Rodrigo MA, Comninellis C (2003) J Electrochem Soc 150:D79
28. Ibl N, Landolt DJ (1968) Electrochem Soc 115:713
29. Czarnetzki LR, Janssen LJJ (1992) J Appl Electrochem 22:315
30. United States Environmental Protection Agency (USEPA) (2001) Implementation guidance for the interim enhanced surface water treatment rule. USEPA, Washington
31. Saravanathamizhan R, Balasubramanian N, Srinivasakannan C (2010) J Model Simul Syst 1:68
32. Tzatchkov VG, Buchberger SG, Martin-Dominguez A (2009) J Environ Eng 135:944
33. Chen T (1967) Anal Chem 39:804
34. Fletcher IJ, Hernrnings P (1985) Analyst 110:695
35. Greef R, Peat R, Peter LM, Pletcher D, Robinson J (1985) Instrumental methods in electrochemistry. Ellis Horwood, Chichester
36. Pickett DJ (1979) Electrochemical reactor design. Elsevier, Amsterdam
37. Trinidad P, Walsh FC (1996) Electrochim Acta 41:493
38. Mascia M, Vacca A, Polcaro AM, Palmas S, Da Pozzo A (2011) J Chem Technol Biotechnol 86:128
39. Tasaka A, Tojo T (1985) J Electrochem Soc 132:1855
40. Saravanathamizhan R, Paranthaman R, Balasubramanian N, Ahmed Basha C (2008) Ind Eng Chem Res 47:2976
41. Levenspiel O (1999) Chemical reaction engineering. Wiley, New York
42. Chao MS (1968) J Electrochem Soc 115:1172